Copper-Induced Conformational Changes in the N-Terminal Domain of the Wilson Disease Copper-Transporting ATPase †

ARTICLE *in* BIOCHEMISTRY · MARCH 2000

Impact Factor: 3.02 · DOI: 10.1021/bi992222j · Source: PubMed

5 AUTHORS, INCLUDING:

Michael DiDonato
Genomics Institute of the Novartis Research …
52 PUBLICATIONS **884** CITATIONS
SEE PROFILE

Lawrence Que
University of Minnesota Twin Cities
451 PUBLICATIONS **25,953** CITATIONS
SEE PROFILE

Copper-Induced Conformational Changes in the N-Terminal Domain of the Wilson Disease Copper-Transporting ATPase†

Michael DiDonato,‡,§,|| Hua-Fen Hsu,⊥ Suree Narindrasorasak,‡ Lawrence Que, Jr.,*,⊥ and Bibudhendra Sarkar*,‡,§

Department of Structural Biology and Biochemistry, The Hospital for Sick Children, Toronto, Ontario M5G 1X8, Canada, Department of Biochemistry, University of Toronto, Toronto, Ontario M5S 1A8, Canada, and Department of Chemistry and Center for Metals in Biocatalysis, University of Minnesota, Minneapolis, Minnesota 55455

Received September 23, 1999; Revised Manuscript Received November 18, 1999

ABSTRACT: The Wilson disease copper-transporting ATPase plays a critical role in the intracellular trafficking of copper. Mutations in this protein lead to the accumulation of a toxic level of copper in the liver, kidney, and brain followed by extensive tissue damage and death. The ATPase has a novel amino-terminal domain (∼70 kDa) which contains six repeats of the copper binding motif GMTCXXC. We have expressed and characterized this domain with respect to the copper binding sites and the conformational consequences of copper binding. A detailed analysis of this domain by X-ray absorption spectroscopy (XAS) has revealed that each binding site ligates copper in the +1 oxidation state using two cysteine side chains with distorted linear geometry. Analysis of copper-induced conformational changes in the amino-terminal domain indicates that both secondary and tertiary structure changes take place upon copper binding. These copper-induced conformational changes could play an important role in the function and regulation of the ATPase in vivo. In addition to providing important insights on copper binding to the protein, these results suggest a possible mechanism of copper trafficking by the Wilson disease ATPase.

Wilson disease (WND)[1] is a major genetic disorder of copper metabolism in humans (*1*). The disease is characterized by the toxic accumulation of copper in various organs but primarily in the liver, kidney, and brain. The gene responsible for the disease resides on chromosome 13 and has been shown to code for a copper-transporting p-type ATPase (ATP7B) (*2*, *3*). The gene is expressed at a high level in the liver and kidney, with a lower level being detected in the lung and placenta (*2*). Recent immunohistochemical studies have shown that the WND ATPase is localized to the trans-Golgi network under steady-state conditions (*4*, *5*). The subcellular distribution of the ATPase can be altered by increasing copper levels. Under elevated copper levels, the ATPase undergoes a reversible, copper-mediated relocalization to both the plasma membrane and a cytoplasmic vesicular compartment which is localized toward the hepatocyte canalicular membrane (*4*, *5*). This copper-induced protein translocation was first characterized in the related copper-transporting P-type ATPase from Menkes disease (*6*). The mechanism by which this translocation event occurs is not understood.

Although similar to other cation-transporting ATPases, the WND ATPase has a novel amino-terminal domain (WCBD) containing six copies of the motif GMTCXXC which are responsible for ligating copper. Between one and three copies of this motif are also present at the amino terminus of bacterial proteins responsible for the transport of metals such as zinc, cadmium, and mercury (*7*). The precise function of this large domain in vivo remains unknown; however, our results suggest a larger role for this domain beyond just binding copper. Previously, it has been shown that the WCBD is able to bind six copper atoms in addition to an array of transition metals, with varying affinities (*8*, *9*). More importantly, copper binding to the WCBD was shown to be cooperative in competition ^{65}Zn binding studies (*8*). Despite these studies, very little is known about the copper binding sites in the WCBD or how the binding of copper affects its structure.

Menkes disease (MNK) is another genetic disorder of copper metabolism which is caused by mutations in a copper-transporting p-type ATPase (ATP7A) which shares a high degree of homology with the WND protein (*10*−*12*). Structural studies on the copper binding domain from the MNK ATPase have been carried out, but it is unclear if these results are representative of the entire domain. These studies have shown that the binding of copper to the second copper binding domain does not significantly alter its structure (*13*). These results are similar to those derived from NMR studies of the fourth copper binding domain from the MNK ATPase

† This work was supported by grants from the Medical Research Council of Canada (MOP-1800) and the U.S. National Science Foundation (DMB9808350).

* Corresponding authors.
‡ The Hospital for Sick Children.
§ University of Toronto.
|| Current address: Department of Molecular Biology, Scripps Research Institute, La Jolla, CA 92037.
⊥ University of Minnesota.

[1] Abbreviations: WND, Wilson disease; BCS, bathocuproinedisulfonic acid; CD, circular dichroism; DTT, dithiothreitol; EXAFS, extended X-ray absorption fine structure; GST, glutathione-*S*-transferase; NAA, neutron activation analysis; Im, imidazole; β-ME, β-mercaptoethanol; TCA, trichloroacetic acid; TGN, trans-Golgi network; TMEDA, *N*,*N*,*N*′,*N*′-tetramethylethylenediamine; WCBD, copper binding domain of Wilson disease copper-transporting ATPase (residues 1−649); XANES, X-ray absorption near-edge structure; XAS, X-ray absorption spectroscopy.

10.1021/bi992222j CCC: $19.00
Published on Web 01/25/2000

with silver bound (*14*). The structures of the apo and silver-(I)-bound proteins are virtually identical, and linear ligation geometry with two cysteine residues is also observed. Linear copper coordination has also been observed in the entire copper binding domain from the MNK ATPase (*15*); however, the copper stoichiometry in this study was not specified. We report a detailed structural analysis of the entire WCBD using various stoichiometries of copper by circular dichroism (CD) and X-ray absorption spectroscopy (XAS). This study has revealed that each binding site in the domain ligates copper in +1 oxidation state using two cysteine side chains accompanied by both secondary and tertiary structural changes in the WCBD upon copper binding. These properties may have biochemical implications for the function of the WCBD in vivo.

EXPERIMENTAL PROCEDURES

Expression and Purification. The cDNA encoding the WCBD which was previously expressed using pGEX-4T-2 (*8*) was subcloned into pGEX-6P-2 (Pharmacia) and expressed in *E. coli* strain BL21(DE3) after induction with IPTG. The fusion protein was present in the soluble fraction and in inclusion bodies. Fusion protein which localized to inclusion bodies was solubilized in 6 M urea and refolded, essentially as described previously (*16*). Refolded fusion protein was combined with the soluble fraction. The resulting mixture was made 1% in Triton X-100 and applied to a glutathione Sepharose 4B column previously equilibrated with TEND-T (20 mM Tris-HCl, pH 8.0, 130 mM NaCl, 1 mM EDTA, 5 mM DTT, 1% Triton X-100). The fusion protein was eluted with TEND-U (20 mM Tris-HCl, pH 8.0, 130 mM NaCl, 1 mM EDTA, 5 mM DTT, 6 M urea). Fractions containing fusion protein were combined and applied to a Q-Sepharose fast flow column, equilibrated with TEND-U. The fusion protein was eluted with a linear salt gradient (130−250 mM NaCl). Peak fractions were analyzed by SDS−PAGE, and those containing fusion protein were pooled and refolded as above. Protein concentration was determined using the BCA protein assay (Pierce) and metal content using NAA. The identity of the expressed protein was confirmed by seven rounds of amino-terminal sequencing.

Removal of GST Moiety. The GST moiety was removed from the fusion protein by incubation with PreScission protease. One unit of PreScission protease (Pharmacia)/mg of fusion protein was added to the protein solution, and the reaction mixture was incubated at 5 °C for 16−48 h. The progress of the cleavage reaction was monitored by SDS−PAGE. Once the reaction was judged complete, the mixture was passed over a glutathione affinity column to remove free GST and the protease (the protease is supplied as a fusion with GST). The flow-through contained the purified WCBD.

Metal Removal. Metal removal from the fusion protein as well as the WCBD was achieved as follows: A solution containing the fusion protein or the WCBD was made 0.5 M in β-ME and incubated at 4 °C for 6−8 h. Following this incubation, the proteins were rapidly precipitated by the addition of TCA to a final concentration of 10%, followed by centrifugation at 3000*g* for 15 min at 4 °C. The protein pellet was resolubilized in 0.5 M Tris base, 6 M urea, 0.5 M β-ME with shaking at 4 °C overnight. After resolubilization, the protein was again precipitated with TCA and resolubilized in 0.5 M Tris, 6 M urea. The protein was then refolded by dialysis against modified refolding buffer (50 mM Tris−acetate, pH 8.0, 20% glycerol) and then refolding buffer without glycerol. The protein concentration was determined by the BCA protein assay (Pierce) and then analyzed for metal content by NAA.

Preparation of Samples for XAS and CD. Fusion protein and WCBD containing various amounts of copper were prepared as follows. DTT was added to act as a reductant in samples of apo-GST-WCBD or apo-WCBD to a final concentration of 1 mM and incubated on ice for 30 min. The required amount of copper (using $CuSO_4$) was then added to achieve the desired final molar ratio of metal/protein and incubated at room temperature for at least 30 min; the DTT present served to reduce the Cu(II) to the Cu(I) oxidation state. A 15-fold molar excess of metal was usually used to achieve full reconstitution of the protein with metal. The unbound metal and DTT were then removed by extensive dialysis against 25 mM ammonium acetate pH 7.5 (25 mM Tris-HCl, pH 8.0, for CD samples). The protein concentration was again confirmed by the BCA protein assay, and metal content was assessed by NAA. All dialysis buffers were purged with argon before use, and dialysis was performed in sealed containers. Typical concentrations of apo-fusion protein used in this procedure were between 1 and 5 mg/mL. XAS samples were lyophilized by first flash-freezing them using a dry ice/acetone bath and then lyophilizing them for 4 days on a Freezemobile 25XL lyophilizer (Virtis).

EXAFS Data Collection and Analysis. The lyophilized proteins were packed into EXAFS sample cells (20 × 2 × 2 mm). X-ray absorption spectra were collected between 8799 and 9726 eV at beamline X9B of the National Synchrotron Light Source (NSLS) at Brookhaven National Laboratory. The protein data were collected in the fluorescence mode at 10−20 K by using a flat Si(220) double-crystal monochromator and a 13-element Ge detector. The monochromator was calibrated using the edge energy of copper foil at 8980.3(3) eV.

The treatment of raw EXAFS data to yield χ is discussed in detail in review articles (*17*, *18*). The *SSExaf*s program was used to extract χ from A_{exp} by using a cubic spline function, including preliminary base line correction and correction of fluorescence data for thickness effects and detector response. General procedures for analysis using the program *SSExaf*s have been presented in other papers (*19*). The refinements reported were on $k^3\chi$ data, and the function minimized was $R = \{\Sigma k^6(\chi_c - \chi)^2/N\}^{1/2}$, where the sum is over N data points between 2 and 14 Å^{-1}.

Single-scattering EXAFS theory allows the total EXAFS spectrum to be described as the sum of shells of separately modeled atoms, e.g.:

$$\chi_c = \Sigma nA[f(k)k^{-1}r^{-2}\exp(-2\sigma^2k^2)\sin(2kr + \alpha(k))]$$

where n is the number of atoms in the shell, $k = [8\pi^2m_e(E - E_0 + \Delta E)/h^2]^{1/2}$, and σ^2 is the Debye−Waller factor (*20*). The amplitude reduction factor (A) and the shell-specific edge shift (ΔE) are empirical parameters that partially compensate for imperfections in the theoretical amplitude and phase functions (*21*). Phase and amplitude functions were theoreti-

cally calculated using a curved-wave formalism (*22*). A variation of FABM (fine adjustment based on models) was used here in the analysis procedure with theoretical phase and amplitude functions (*23*). In each shell, two parameters were refined at one time (r and n or σ^2), while A and ΔE values were determined by using a series of crystallographically characterized model complexes, namely, $[Cu(SC_{10}H_{13})_2]^-$, $[Cu(Im)_4]^{2+}$, and $[Cu_2(TMEDA)_2(OH)_2]^{2+}$. The following A and ΔE values were used for our fits: for N/O, 0.21 and 9.9; for S, 0.57 and 6.0; for Cu, 0.70 and 1.8. The fitting results indicate the average metal−ligand distances, the type and the number of scatterers, and the Debye−Waller factors which can be used to evaluate the distribution of Cu−ligand bond lengths in each shell. The EXAFS goodness of fit criterion applied here is

$$\epsilon^2 = [(N_{idp}/\nu)\Sigma(\chi_c - \chi)^2/{\sigma_{data}}^2]/N$$

as recommended by the International Committee on Standards and Criteria in EXAFS (*24, 25*) where ν is the number of degrees of freedom, calculated as $\nu = N_{idp} - N_{var}$, N_{idp} is the number of independent data points, and N_{var} is the number of variables that are refined. N_{idp} is calculated as $N_{idp} = 2\Delta k\Delta R/\pi + 2$, and σ_{data} is the estimated uncertainty of the data (usually set at 1) (*26*). The use of ϵ^2 as the criterion for the goodness of fit allows us to compare fits using different numbers of variable parameters.

Conformational Analysis of WCBD by CD. Samples for CD analysis containing various stoichiometries of copper were prepared as described above and analyzed on a Jasco J-720 spectropolarimeter. For analysis of changes in secondary structure, samples were loaded into a 0.1 cm path length CD cell, and spectra were recorded from 300 to 190 nm. For analysis of changes in tertiary structure, samples were loaded into a 2 cm path length CD cell and spectra recorded from 400 to 250 nm. The spectra were corrected for the contribution of the buffer and noise reduced, and the data were converted to molar ellipticity using the software supplied with the spectrometer. Molar ellipticity values per residue were calculated by dividing the molar ellipticity by the number of residues in the WCBD (649 residues). The concentration of the protein solution was 14.5 μM.

RESULTS

CD Spectral Analysis. Samples of the WCBD containing two, four, or six bound copper atoms were prepared by the addition of copper to the apo-WCBD as described previously, and CD spectra were obtained. Addition of increasing amounts of copper to the WCBD resulted in a progressive increase in secondary structure (Figure 1A). The magnitude of the change is greatest between the apo-WCBD and the 2:1 complex and to a lesser extent from the 4:1 complex to the 6:1 complex.

These secondary structure changes are paralleled by drastic changes in the tertiary structure as well (Figure 1B,C). In the aromatic region, large changes in magnitude and line shape are observed with increasing copper content. For example, the ellipticity at 260 nm increases on going from the apo-WCBD to the 2:1 complex and becomes negative from the 2:1 complex to the 4:1 and 6:1 complexes. The ellipticity also increases at 290 nm as copper ions are added, with the largest change occurring between the 2:1 and 4:1

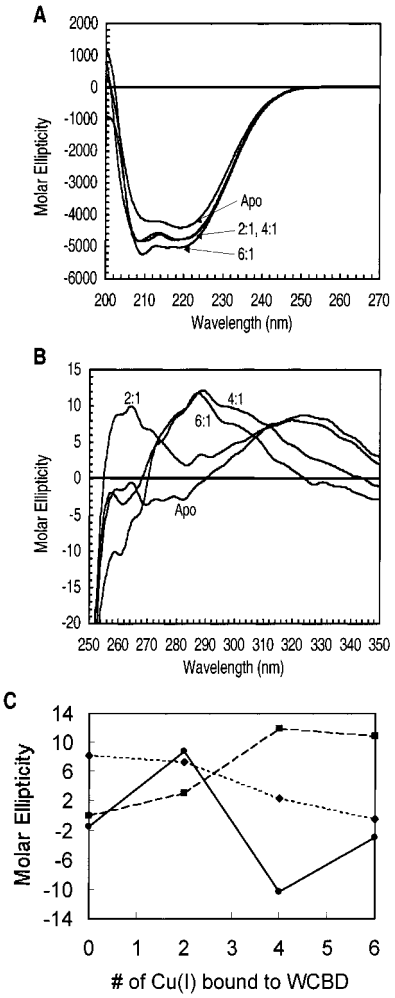

FIGURE 1: Copper-induced conformational changes in the WCBD as monitored by CD spectroscopy. Samples of apo-WCBD were reconstituted with the indicated ratio of copper as determined using NAA and the BCA protein assay. Spectra were recorded as described under Experimental Procedures. (A) Secondary structure region. (B) Tertiary structure region. (C) Molar ellipticity in the WCBD as a function of the number of Cu(I) bound per protein: molar ellipticity at 260 (●), 290 (■), and 330 (◆) nm.

samples. Last, there is a progressive loss in ellipticity at ~330 nm as more copper is bound. Ellipticity in this region can be attributed to the presence of disulfide bonds which are present in the absence of bound copper (*27*). As copper is bound, the cysteine residues become involved in copper ligation and therefore are unavailable for disulfide bond formation, resulting in a decrease in the ellipticity at 330 nm. The WCBD contains six additional cysteine residues which are not part of the GMTCXXC repeats. The absence of any ellipticity at 330 nm in the fully reconstituted samples suggests that these residues exist as free sulfhydryls.

The increase in secondary structure upon copper binding indicates that the structure of the WCBD may be stabilized as copper becomes bound. The 2:1 and 4:1 copper complexes are nearly identical in secondary structure, but their tertiary structure spectra are very different. This implies that the structural organization of the WCBD is being altered as each metal-binding domain becomes progressively occupied with copper. These tertiary structure changes could be the basis for the cooperative binding of copper which has been observed in competition ^{65}Zn blotting experiments (*8*).

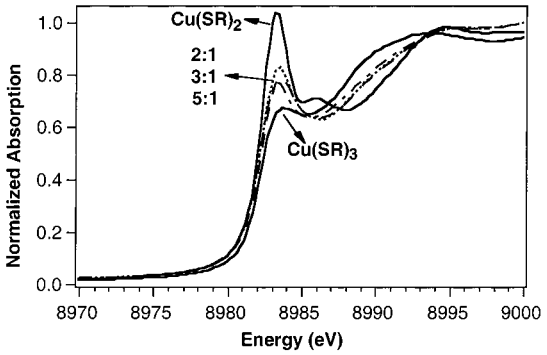

FIGURE 2: Normalized Cu K-edge XANES spectra of WCBD and Cu(I)−thiolate model compounds. $Cu(SR)_2$: $[Cu(SC_{10}H_{13})_2]^-$, $Cu(SR)_3$: $[Cu(SC_6H_5)_3]^{2-}$; the ratio of Cu to protein = 2:1 (dotted line), 3:1 (dashed line), and 5:1 (dotted and dashed line).

Analysis of X-ray Absorption Spectroscopic Data. To determine if the conformational changes induced by Cu(I) binding as detected by CD are reflected in the copper coordination environments, XAS spectra at the Cu K-edge were obtained for three samples of WCBD with Cu:protein stoichiometries of 2:1, 3:1, and 5:1. The copper content for each sample was determined by metal analysis. All three samples exhibit a near-edge absorption (XANES) feature at 8983.5(3) eV, consistent with the 1s→4p transition of a Cu(I) center (Figure 2) (*28, 29*). Previously reported data on structurally characterized synthetic Cu(I) complexes show that the shape of this 8983.5(3) eV transition varies as a function of Cu(I) geometry; digonal sites have intense and well-resolved peaks, while tetrahedral sites have a feature that is more amorphous. For all the WCBD samples, there is a resolved peak at 8983.5(3) eV, but with an intensity that is somewhat weaker than those of digonal Cu(I) thiolate compounds but stronger than those of corresponding trigonal complexes. The intermediate nature of the XANES feature suggests that the Cu(I) site in WBCD is distorted from the ideal linear geometry of a two-coordinate Cu(I) center with a S−Cu−S angle between 120° and 180°. It is interesting to note that the shape of the XANES feature appears independent of Cu stoichiometry, implying that all the Cu(I) sites of the protein are quite similar.

The analysis of the EXAFS data for the three samples supports the conclusions derived from the XANES data and provides useful metrical information. Figure 3 shows the experimental data and corresponding Fourier-transformed spectra of WCBD with 2:1, 3:1, and 5:1 Cu-to-protein ratios. All three samples give rise to very similar spectra, suggesting that the geometry of the Cu sites is not perturbed dramatically with different amounts of copper bound to WCBD.

The r'-space spectra for all samples exhibit a prominent feature centered at $r' = 1.8$ Å and a minor peak at $r' = 2.3$ Å ($r \sim r' + 0.4$ Å). As summarized in Table 1, the best fit for these features in all samples consists of one shell of two S scatterers at 2.18 ± 0.01 Å (fit 2). Single-shell fits with one or three S atoms afforded poorer goodness-of-fit values (fits 1 and 3). The Cu−S distance of 2.18 Å is most consistent with the presence of a two-coordinate Cu binding site in WCBD. Linear mononuclear two-coordinate Cu(I)−thiolate complexes have been found to have Cu−S distances of 2.14−2.15 Å (*30, 31*), while three-coordinate complexes have Cu−S bonds of 2.26−2.28 Å (*32*−*35*). Bent two-coordinate Cu sites, found in Cu(I)−thiolate clusters, possess intermediate Cu−S distances of 2.16−2.20 Å (*33*−*35*). As a result of this comparison, the Cu−S distance of 2.18 ± 0.01 Å in WCBD matches those found in Cu(I)−thiolate clusters with bent two-coordinate sites and strongly suggests

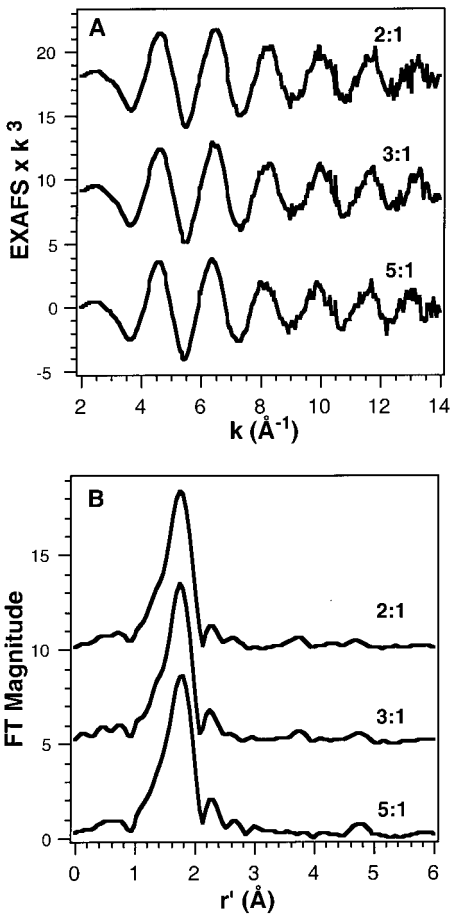

FIGURE 3: EXAFS of WCBD with the indicated ratio of copper to protein. (A) *k*-space spectra. (B) r'-space spectra.

Table 1: EXAFS Analysis of WCBD with 2:1 (Top), 3:1 (Middle), and 5:1 (Bottom) Cu to Protein Ratios[a]

	Cu−S			Cu−X			
fit no.	*n*	*r* (Å)	σ^2	*n*	*r* (Å)	σ^2	$\epsilon^2 \times 10^4$
			2:1				
1	3	2.17	0.011				5.7
2	**2**	**2.17**	**0.007**				**2.6**
3	1	2.17	0.002				5.3
4	2	2.15	0.008	1N/O	2.07	−0.001	2.2
5	2	2.17	0.007	1S	2.60	0.060	2.6
6	2	2.17	0.007	1Cu	2.56	0.033	3.0
			3:1				
1	3	2.17	0.012				5.9
2	**2**	**2.17**	**0.007**				**3.3**
3	1	2.17	0.003				5.4
4	2	2.15	0.008	1N/O	2.05	−0.002	2.7
5	2	2.17	0.007	1S	2.60	0.060	3.5
6	2	2.17	0.007	1Cu	2.55	0.030	3.7
			5:1				
1	3	2.19	0.012				4.9
2	**2**	**2.19**	**0.008**				**3.3**
3	1	2.19	0.003				6.2
4	2	2.17	0.009	1N/O	2.08	−0.001	3.4
5	2	2.19	0.008	1S	2.78	0.027	3.2
6	2	2.18	0.008	1Cu	2.54	0.023	3.2

[a] Fourier transform range $k = 2-14$ Å^{-1}; back-transform range $r' = 1-2.8$ Å.

that the Cu(I) sites in WCBD have a distorted digonal geometry.

The appearance of a weak feature at $r' = 2.3$ Å in the r'-space spectra raises the possibility of additional scatterers in the copper coordination environment. However, attempts to add another shell of scatterers to the S shell at 2.18 ± 0.01 Å did not improve the one-shell fit (Table 1, fits 4−6). Furthermore, the added scatterer, whether it be O/N, S, or Cu, was associated with negative or unreasonably large Debye−Waller factors. Similar results were obtained with various back-transform ranges (e.g., $r' = 1-2.5$ and 1−2.8 Å). We attempted to introduce a S scatterer at 2.4 Å by analogy to Atx1, but this distance lengthened to 2.6−2.8 Å in the course of the refinement. Thus, it is unlikely that a third scatterer is present in the copper coordination sphere. Last, there are weak outer sphere features in the $r' = 3-5$ Å region which may arise from trace Cu metal contamination.

DISCUSSION

The XAS and CD studies of the WCBD with substoichiometric amounts of copper have provided a wealth of detailed structural information on this unique domain. All copper atoms appear to be ligated by two sulfur residues in a distorted linear arrangement with a Cu−S distance of 2.17−2.19 Å. A Cu−S distance of 2.16 Å has also been found in an EXAFS study of the related Menkes disease protein (MNK) (*15*) which has the same copper binding sequence motif (MTCXXC) as the WCBD, suggesting similar Cu(I) coordination environments for the two proteins. In contrast, a different copper coordination environment has been reported for Atx1, the copper chaperone protein found in yeast which also has the same copper binding sequence motif. Atx1 has two sulfur scatterers at 2.25 Å and a third sulfur scatterer at 2.40 Å, implicating a three-coordinate copper site (*36*). The third sulfur scatterer was originally proposed to be the methionine residue in the conserved sequence, but this residue is found to be quite distant from the linear digonally coordinated metal center in the recent crystallographic study of the Hg derivative of Atx1 (*37*). An alternative suggestion for the third sulfur scatterer is the sulfur of the glutathione present in the Atx1 sample preparations for the EXAFS studies. Our samples of WCBD were prepared in the presence of a thiol reductant, DTT, but our data analysis does not indicate the presence of a third S scatterer in the Cu coordination sphere and strongly suggests that the Cu(I) environments of WCBD and Atx1 differ. Cox17, another copper chaperone protein but one with a copper binding sequence different from that of Atx1 and WCBD, also shows a Cu−S distance of 2.26 Å, indicating a three-coordinate copper binding site (*38*). There thus appears to be a range of possible Cu(I) binding modes for this group of proteins.

The EXAFS analyses for MNK and Cox17 provide some evidence for copper cluster formation. For MNK, an outer sphere feature at $r' = 2.3$ Å could be fit with a copper scatterer with a Cu−Cu distance of 2.6 Å (*14*). For Cox17, a Cu−Cu distance of 2.7 Å was found (*38*). These results suggest that the individual copper sites in these proteins may come together and form dinuclear cores with single atom bridges, similar to the $Cu_2(\mu\text{-}SR)_2$ site found in cytochrome *c* oxidase (Cu−Cu ∼ 2.5 Å) (*39*). We were unable to fit such a copper scatterer at 2.5 Å in our data analysis of WBCD and thus do not have evidence for the formation of such copper clusters in this protein.

Nevertheless, our CD studies have shown that the binding of copper to the WCBD does indeed trigger a series of secondary and tertiary structural changes in the domain. Our EXAFS results indicate that these structural changes are not centered around the copper binding sites, since the EXAFS spectra (Figure 3) clearly show that the coordination environment around the copper atoms does not change upon the binding of successive copper atoms. It is likely that the ligation of copper by WCBD results in structural changes around the metal binding site which are transmitted to other parts of the molecule through the protein backbone. These subtle changes could then lead to more substantial tertiary structure changes elsewhere in the domain as is observed in the CD spectra (Figure 1B). Alternatively, the observed structural changes could result from the disruption of disulfide bonds which are present in the absence of metal. The WCBD contains 18 cysteine residues, 12 of which are conserved. In the absence of copper, some of these may form disulfide bonds. The presence of ellipticity at 330 nm in the CD spectra of the apo-WCBD strongly suggests the presence of disulfide bonds. The progressive loss of this feature as copper binds suggests that these disulfide bonds are disrupted, leading to the structural changes observed in the domain.

These conformational changes may also play a key role in the in vivo regulation of the ATPase. A hypothetical model is presented in Figure 4 which is supported by the structural data presented here as well as several functional studies on the ATPase. In this model, the Wilson disease ATPase (WND) resides in the TGN under normal physiological conditions where it pumps copper into the TGN lumen. When unoccupied with copper, the amino-terminal domain would interact with other cytosolic loops of the protein, preventing the transport of copper. The binding of copper triggers conformational changes in the WCBD which disrupt its interaction with the rest of the protein and initiate the transport cycle. When the cytoplasmic concentrations of copper rise, additional copper binding sites become occupied, leading to further conformational change. The binding of copper to these additional sites may occur in a cooperative manner (*8*). These conformational changes may act as a trigger for the translocation of the protein from the TGN to the plasma membrane as well as a vacuolar compartment. At the plasma membrane, the WND ATPase would function to expel excess copper from the hepatocyte. Copper pumped into a vacuole by the WND ATPase could be excreted by the hepatocyte via an alternate pathway. A recent study has shown that these vacuoles are localized toward the canalicular membrane and may provide a route for the excretion of copper into the bile by fusing with the canalicular membrane (*5*). As the cytoplasmic concentration of copper decreases, the N-terminal domain becomes progressively unoccupied, and the ATPase is recycled to the TGN.

Several studies have made it clear that in both the Menkes and Wilson disease proteins, not all the metal binding repeats are needed to allow transport activity (*4*, *6*, *40*). These observations suggest that the remaining repeats may have

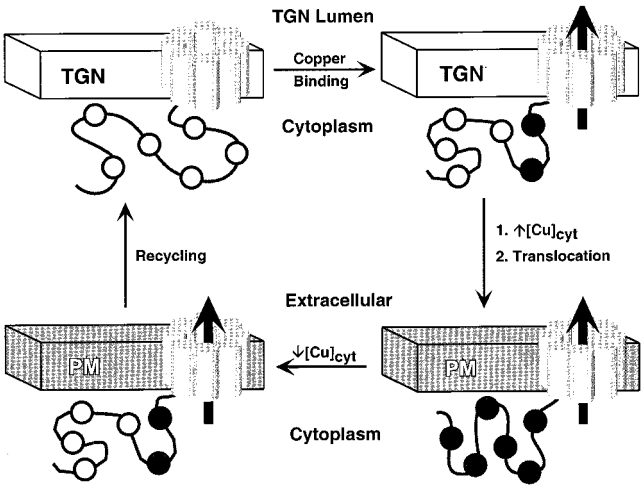

FIGURE 4: Hypothetical model for the function of WND in vivo. Under normal conditions, the WND protein is localized in the trans-Golgi network (TGN). When not occupied with copper, the metal binding domain interacts with the cytosolic loops of the ATPase. Binding of copper to the metal binding repeats closest to the transmembrane segments results in a conformational change which stimulates the phosphorylation of the ATPase and initiation of copper transport into the TGN lumen. Under conditions of elevated cytoplasmic copper, all of the metal binding repeats become occupied with copper resulting in further conformational changes and the translocation of the WND from the TGN to the plasma membrane (PM). At the PM, the WND protein would pump copper from the cytoplasm into the extracellular space, lowering the cytoplasmic concentration of copper. As intracellular copper levels decrease, the metal binding repeats become progressively unoccupied, and the WND is recycled back to the TGN.

an alternate role such as helping to regulate the activity of the protein. However, recent studies have indicated that this may not be the case in the Menkes protein. These studies have shown that at least one of the C-terminal-most metal binding domains is needed to allow the copper-induced translocation of the ATPase (*41*). These authors have also shown that the first four metal repeats could be eliminated without loss of copper-induced relocation; mutation of the remaining two metal repeats abolished its response to copper. This study did not address the effect of these mutations on copper transport activity.

These observations are in sharp contrast to similar studies performed in the WND protein which show that the first five metal repeats could be mutated without loss of copper transport activity (*42)*. Taken together, these studies illustrate that the metal repeats are not functionally equivalent and the metal binding domains of the Menkes and Wilson proteins do not function in the same manner. In light of this, the results of the study by Strausak et al. (*41)* cannot be extrapolated easily to the Wilson disease protein. The differences which exist in the metal binding domains for the Wilson and Menkes disease proteins may account for their functional differences. The greatest of these is a 78 amino acid deletion in the Wilson disease protein (relative to the Menkes protein) between the first and second metal binding repeats (*2*). The deletion of this region could have a great effect on the copper binding properties of the WCBD and hence the biological function of the entire protein. If this deletion is responsible for imparting a cell-specific function to the ATPase, it may help to explain the functional differences between the two domains as well as the existence of two separate gene products which carry out the same essential function.

ACKNOWLEDGMENT

We thank Professor Robert C. Scarrow for generously providing *SSExafs*. We thank Kui Chen, Dr. Raymond Y. N. Ho, and Dr. Mark Reynolds for assistance with data collection. XAS data for the model compounds were generously provided by Professors James E. Penner-Hahn for $[Cu(SC_{10}H_{13})_2]^-$ and Robert A. Scott for $[Cu(SC_6H_5)_3]^{2-}$ and $[Cu(Im)_4]^{2+}$. XAS data were collected at X9B at National Synchrotron Light Source at Brookhaven National Laboratory (NSLS) and Stanford Synchrotron Radiation Laboratory (SSRL). Beamline X9B at NSLS is supported by the National Institutes of Health (RR-001633), and SSRL operation is funded by the U.S. Department of Energy with additional support from the NIH Research Resource program. We thank Dr. Britt Hedman of SSRL for her valuable assistance at SSRL.

REFERENCES

1. DiDonato, M., and Sarkar, B. (1997) *Biochim. Biophys. Acta 1360*, 3−16.
2. Bull, P. C., Thomas, G. R., Rommens, J. M., Forbes, J. R., and Cox, D. W. (1993) *Nat. Genet. 5*, 327−337.
3. Tanzi, R. E., Petrukhin, K., Chernov, I., Pellequer, J. L., Wasco, W., Ross, B., Romano, D. M., Parano, E., Pavone, L., Brzustowicz, L. M., Devoto, M., Peppercorn, J., Bush, A. I., Sternlieb, I., Piratsu, M., Gusella, J. F., Evgrafov, O., Penchaszadeh, G. K., Honig, B., Edelman, I. S., Soares, M. B., Scheinberg, I. H., and Gilliam, T. C. (1993) *Nat. Genet. 5*, 344−350.
4. Hung, I. H., Suzuki, M., Yamaguchi, Y., Yuan, D. S., Klausner, R. D., and Gitlin, J. D. (1997) *J. Biol. Chem. 272*, 21461−21466.
5. Schaefer, M., Hopkins, R. G., Failla, M. L., and Gitlin, J. D. (1999) *Am. J. Physiol. Gastrointest. L 39*, G639−G646.
6. Petris, M. J., Mercer, J. F., Culvenor, J. G., Lockhart, P., Gleeson, P. A., and Camakaris, J. (1996) *EMBO J. 15*, 6084−6095.
7. Silver, S., and Phung, L. T. (1996) *Annu. Rev. Microbiol. 50*, 753−789.
8. DiDonato, M., Narindrasorasak, S., Forbes, J. R., Cox, D. W., and Sarkar, B. (1997) *J. Biol. Chem. 272*, 33279−33282.
9. Lutsenko, S., Petrukhin, K., Cooper, M. J., Gilliam, C. T., and Kaplan, J. H. (1997) *J. Biol. Chem. 272*, 18939−18944.
10. Chelly, J., Tumer, Z., Tønnesen, T., Petterson, A., Ishikawa-Brush, Y., Tommerup, N., Horn, N., and Monaco, A. P. (1993) *Nat. Genet. 3*, 14−19.
11. Mercer, J. F., Livingston, J., Hall, B., Paynter, J. A., Begy, C., Chandrasekharappa, S., Lockhart, P., Grimes, A., Bhave, M., Siemieniak, D., and Glover, T. W. (1993) *Nat. Genet. 3*, 20−25.
12. Vulpe, C., Levinson, B., Whitney, S., Packman, S., and Gitschier, J. (1993) *Nat. Genet. 3*, 7−13.
13. Harrison, M. D., Meier, S., and Dameron, C. T. (1999) *Biochim. Biophys. Acta 1453*, 254−260.
14. Gitschier, J., Moffat, B., Reilly, D., Wood, W. I., and Fairbrother, W. J. (1998) *Nat. Struct. Biol. 5*, 47−54.
15. Ralle, M., Cooper, M. J., Lutsenko, S., and Blackburn, N. J. (1998) *J. Am. Chem. Soc. 120*, 13525−13526.
16. Dombroski, A. J., Walter, W. A., Record, M. T., Jr., Siegele, D. A., and Gross, C. A. (1992) *Cell 70*, 501−512.
17. Scott, R. A. (1985) *Methods Enzymol. 11*, 414−459.
18. Teo, B.-K. (1981) in *EXAFS Spectroscopy, Techniques and Applications* (Teo, B.-K., and Joy, D. C., Eds.) pp 13−58, Plenum, New York.

19. Scarrow, R. C., Trimitsis, M. G., Buck, C. P., Grove, G. N., Cowling, R. A., and Nelson, M. J. (1994) *Biochemistry 33*, 15023−15035.
20. Scarrow, R. C., Maroney, M. J., Palmer, S. M., Roe, A. L., Que, L., Jr., Salowe, S. P., and Stubbe, J. (1987) *J. Am. Chem. Soc. 109*, 7857−7864.
21. Teo, B.-K., and Lee, P. A. (1979) *J. Am. Chem. Soc. 101*, 2815−2832.
22. McKale, A. G., Veal, B. W., Paulikas, A. P., Chan, S.-K., and Knapp, G. S. (1988) *J. Am. Chem. Soc. 110*, 3763−3768.
23. Teo, B.-K., Antonio, M. R., and Averill, B. A. (1983) *J. Am. Chem. Soc. 105*, 3751−3762.
24. Bunker, G., Hasnain, S. S., and Sayers, D. (1991) in *X-ray Absorption Fine Structure* (Hasnain, S. S., Ed.) pp 751−770, Ellis Horwood, New York.
25. Riggs-Gelasco, P. J., Stemmler, T. L., and Penner-Hahn, J. E. (1995) *Coord. Chem. Rev. 144*, 245−286.
26. Stern, E. (1993) *Phys. Rev. B 48*, 9825−9827.
27. Wingfield, P. T., and Pain, R. H. (1996) in *Current Protocols in Protein Science* (Coligan, J. E., Dunn, B. M., Ploegh, H. L., Speicher, D. W., and Wingfield, P. T., Eds.) pp 7.6.1−7.6.23, John Wiley & Sons, Inc., New York.
28. Kau, L.-S., Spira-Solomon, D. J., Penner-Hahn, J. E., Hodgson, K. O., and Solomon, E. I. (1987) *J. Am. Chem. Soc. 109*, 6433−6442.
29. Pickering, I. J., George, G. N., Dameron, C. T., Kurz, B., Winge, D. R., and Dance, I. G. (1993) *J. Am. Chem. Soc. 115*, 9498−9505.
30. Koch, S. A., Fikar, R., Millar, M., and O'Sullivan, T. (1984) *Inorg. Chem. 23*, 122−124.
31. Fujisawa, K., Imai, S., Kitajima, N., and Moro-oka, Y. (1998) *Inorg. Chem. 37*, 168−169.
32. Coucouvanis, D., Murphy, C. N., and Kanodia, S. K. (1980) *Inorg. Chem. 19*, 2993−2998.
33. Dance, I. G., Bowmaker, G. A., Clark, G. R., and Seadon, J. K. (1983) *Polyhedron 2*, 1031−1043.
34. Dance, I. G. (1986) *Polyhedron 5*, 1037−1104.
35. Bowmaker, G. A., Clark, G. R., Seadon, J. K., and Dance, I. G. (1984) *Polyhedron 3*, 535−544.
36. Pufahl, R. A., Singer, C. P., Peariso, K. L., Lin, S.-J., Schmidt, P. J., Fahrni, C. J., Culotta, V. C., Penner-Hahn, J. E., and O'Halloran, T. V. (1997) *Science 278*, 853−856.
37. Rosenzweig, A. C., Huffman, D. L., Hou, M. Y., Wernimont, A. K., Pufahl, R. A., and O'Halloran, T. V. (1999) *Structure 7*, 605−617.
38. Srinivasan, C., Posewitz, M. C., George, G. N., and Winge, D. R. (1998) *Biochemistry 37*, 7572−7577.
39. Blackburn, N. J., Vries, S. D., Barr, M. E., Houser, R. P., Tolman, W. B., Sanders, D., and Fee, J. A. (1997) *J. Am. Chem. Soc. 119*, 6135−6143.
40. Nagano, K., Nakumura, K., Urakami, K. I., Umeyama, K., Uchiyama, H., Koiwai, K., Hattori, S., Yamamoto, T., Matsuda, I., and Endo, F. (1998) *Hepatology 27*, 799−807.
41. Strausak, D., Fontaine, S. L., Hill, J., Firth, S. D., Lockhart, P. J., and Mercer, J. F. (1999) *J. Biol. Chem. 274*, 11170−11177.
42. Forbes, J. R., Hsi, G., and Cox, D. W. (1999) *J. Biol. Chem. 274*, 12408−12413.

BI992222J